Atomic layer deposited high-k nanolaminate capacitors

S.W. Smith *, K.G. McAuliffe, J.F. Conley Jr.

School of Electrical Engineering and Computer Science and Department of Materials Science, Oregon State University, USA

ARTICLE INFO

ABSTRACT

Al_2O_3–Ta_2O_5 nanolaminate films were prepared via atomic layer deposition (ALD) on silicon with a single overall composition and thickness, but with a varying number of Al_2O_3/Ta_2O_5 bilayers. The composition of the films was roughly 57% Al_2O_3 and 43% Ta_2O_5 and the total film thickness was held at ~58 nm, while the number of bilayers was varied from 3 to 192 by changing the target bilayer thickness from ~19.2 nm to ~0.3 nm. Varying the number of bilayers was found to impact electrical properties. Although, almost all laminate films exhibited leakage, breakdown, hysteresis, and overall dielectric constant intermediate between pure Al_2O_3 and Ta_2O_5 films, laminates with few bilayers exhibited leakage current density lower than Al_2O_3 over the range of ~3.5–4.5 MV/cm. Select samples annealed at temperatures from 400 to 900 °C were compared with as-deposited laminates. Annealing the laminate films at low temperatures improved leakage and breakdown while higher temperature anneals degraded both leakage and breakdown but improved the effective dielectric constant. A figure of merit was used to evaluate the overall ability of the various films to store charge. It was found that the few bilayer laminates were ranked higher than the many bilayer laminates as well as above both the pure Ta_2O_5 and pure Al_2O_3 films. These results indicate that even for a fixed overall composition, the electrical properties of a nanolaminate can be adjusted by varying the number of bilayers.

1. Introduction

Nanolaminate dielectric films [1–9] offer the possibility of tailoring the electrical properties of dielectric stacks for applications such as the tunnel dielectric for MIM diodes, storage capacitors [10], non-volatile memories [11], and amorphous oxide semiconductor based transparent thin film transistors (TTFTs) which typically employ gate dielectrics with an equivalent SiO_2 thickness of ~100 nm [12,13]. Deposition of nanolaminates requires atomic level control and the intended applications often require high conformality. An ideal technique for synthesis of multiple oxide nanolaminate films is atomic layer deposition (ALD) [1–9]. In atomic layer deposition (ALD), precursor and oxidation gases are introduced into the reaction chamber alternately, rather than simultaneously [14,15]. The separation of precursors allows film growth to take place through self limiting surface reactions, resulting in atomic scale control and inherently high conformality.

Nanolaminates deposited via ALD have been shown to display properties that are not only a function of composition but depend upon the laminate structure as well. For example, Kukli et al. [2,3] have shown that leakage, permittivity, and charge storage in ALD ZrO_2–Ta_2O_5 and HfO_2–Ta_2O_5 laminates depends not only on the overall composition, as determined by the composition ratio of

the bilayers in the laminate, but also on the bilayer thickness since the spatially confined bilayers influence the crystal structure of as-deposited HfO_2 and ZrO_2.

Kattelus et al. [1] deposited amorphous Ta_2O_5–Al_2O_3 laminates of 70–100 nm total thickness via ALD using $AlCl_3$ and $TaCl_5$ as metal precursors. Composition was adjusted between 20% and 60% Ta_2O_5 by changing the thickness ratio of the alternating Al_2O_3 and Ta_2O_5 layers. They reported that these nanolaminates exhibited dielectric constant and leakage intermediate between the pure films with deviation from pure Al_2O_3 properties primarily for Ta contents above 30%.

In this study, amorphous Ta_2O_5–Al_2O_3 laminates were deposited via ALD using $Al(CH_3)_3$ and $TaCl_5$ as metal precursors and water as an oxidant. By using a single target thickness and overall composition (approximately 57% Al_2O_3/43% Ta_2O_5, based on the bilayer thickness ratio) and varying only the numbers of Ta_2O_5/Al_2O_3 bilayers, the impact of the bilayer thickness and the total number of interfaces on dielectric properties is investigated without interference from changes in overall composition or crystal structure. To explore the influence of crystallization on the laminates, select samples were annealed in an inert atmosphere. Long-range order was measured by X-ray diffraction, dielectric constant and hysteresis by capacitance vs. voltage (C–V), and leakage and breakdown by current vs. voltage (I–V). It was found that despite the fixed overall target composition, varying the number/thickness of the bilayers had an impact on electrical properties. Samples with

* Corresponding author.
E-mail address: smithsea@onid.orst.edu (S.W. Smith).

thinner (more numerous) bilayers tended towards higher effective dielectric constant, but higher leakage current than few (thick) bilayer samples. While almost all samples exhibited electrical characteristics intermediate between single layer Al_2O_3 or Ta_2O_5 films, several of the samples with fewer and thicker bilayers exhibited leakage current density lower than that of Al_2O_3 over the range of ~3.5–4.5 MV/cm. Comparing the samples using a charge storage figure of merit [2,3] revealed these few (thick) bilayer films to be ranked higher than the many bilayer laminates as well as both the pure Ta_2O_5 and pure Al_2O_3 films. These results indicate that even for a fixed overall composition, varying the number of bilayers can be used to tailor the electrical properties of a nanolaminate dielectric.

2. Experimental details

ALD was performed using a commercial Picosun Sunale R-150 hot-wall flow-through ALD reactor. About 150 mm p type $\langle 1\,0\,0 \rangle$ silicon substrates with resistivities of ~12–16 Ω cm were used. Si wafers were cut into 25 mm × 25 mm coupons and cleaned using a standard acetone/isopropyl alcohol/DI water rinse. Immediately prior to deposition, samples were etched in buffered HF in order to minimize the native oxide.

Ta_2O_5 was deposited using $TaCl_5$ and H_2O. A single ALD cycle for Ta_2O_5 consisted of 0.5 s $TaCl_5$ pulse/2 s N_2 purge/0.2 s H_2O/2 s N_2 purge. The deposition rate of Ta_2O_5 was about 0.064 nm/cycle.

Al_2O_3 was deposited using alternating exposures to trimethyl aluminum (TMA, $Al(CH_3)_3$) and H_2O. A single ALD Al_2O_3 cycle consisted of 0.1 s TMA pulse/2 s N_2 purge/0.1 s H_2O pulse/2 s N_2 purge. The deposition rate of Al_2O_3 was about 0.086 nm/cycle.

Fig. 1. Cross sectional schematic of MOS device structure. Overall thickness is fixed at approximately 58 nm and is maintained for various numbers of bilayers by adjusting the bilayer compensate.

Nanolaminate films were deposited at 300 °C (within the ALD temperature window of both processes) and are comprised of stacked pairs of Al_2O_3/Ta_2O_5 layers which are referred to as bilayers, Fig. 1. In all laminate samples, Al_2O_3 was deposited first forming an interface with the Si substrate and Ta_2O_5 last as the top layer. The nominal total thickness of the array (Table 1) was ~58 nm and consisted of a total of 384 ALD cycles each of Al_2O_3 and Ta_2O_5. Use of a ~58 nm film allowed the individual layer thickness to be varied by nearly an order of magnitude. The target bilayer thickness was varied between ~0.3 nm and 19.2 nm. The number of bilayers was varied between three, consisting of 128 ALD cycles (~11.0 nm) of Al_2O_3 followed by 128 cycles (~8.2 nm) of Ta_2O_5, repeated three times and 192, consisting of 2 cycles (~0.18 nm) of Al_2O_3 followed by 2 cycles (~0.12 nm) of Ta_2O_5, repeated 192 times). Note that individual layer thicknesses as well as the total thickness of the laminate films were not measured, but are calculated based on the deposition per cycle times the total number of cycles. It is assumed that the deposition rate holds steady even for few cycle depositions. Thus, based on the differences in deposition rate (0.064 nm per cycle for Ta_2O_5 and 0.086 nm per cycle for Al_2O_3) and the equal number of cycles, the bilayer composition as well as the overall composition of the film is assumed to be ~57% Al_2O_3/43% Ta_2O_5. As a control, 60 nm thick single layer Al_2O_3 and 53.5 nm Ta_2O_5 samples were deposited, with thicknesses confirmed by a Gaertner Scientific 632.8 nm wavelength ellipsometer. A scanning electron microscope (SEM) image was taken using a Quanta 3D dual beam SEM (FIB)) to confirm the discrete layering. The number of bilayers, bilayer structure (number of ALD cycles each of Al_2O_3 and Ta_2O_5 in a bilayer), target Al_2O_3 layer, Ta_2O_5 layer, and total bilayer thicknesses of the samples are displayed in Table 1.

Isochronal rapid thermal annealing was performed on select films for 10 min at 400 °C, 700 °C, 800 °C or 900 °C in an inert Ar ambient. The extent of long range crystalline order in the samples was assessed via X-ray diffraction (XRD) on a Bruker AXS D8 discover using (Cu kα λ = 1.54 nm).

Aluminum dots of ~160 μm, 100 μm, and 70 μm diameter were formed by thermally evaporating aluminum through a shadow mask in order to define metal/oxide/silicon (MOS) capacitor structures. The substrates were unheated during deposition and no post-deposition anneal was performed. The backsides of these substrates were also coated with aluminum to improve backside contact. Leakage current density was measured at an electric field of 1 MV/cm and 4 MV/cm using an Agilent 4155 semiconductor parameter analyzer with long integration time. Breakdown strength was determined from a 1 V/s ramped gate bias sweep. Capacitance vs. voltage (C–V) analysis was performed at 100 kHz using an Agilent 4980A LCR meter. C–V measurements were made by sweeping the DC bias from inversion to accumulation and then back again. Hysteresis (ΔV_{hys}) was determined using the flatband voltage shift ($\Delta V_{fb}(acc \rightarrow Inc.) - \Delta V_{fb}(Inc. \rightarrow acc)$) between the

Table 1
Summary of laminate and pure material samples deposited.

# of Bilayers/film	Bilayer structure		Target Al_2O_3 layer thickness (nm)[a]	Target Ta_2O_5 layer thickness (nm)[a]	Target bilayer thickness (nm)[a]
	Cycles Al_2O_3	Cycles Ta_2O_5			
192	2	2	0.18	0.12	0.3
48	8	8	0.7	0.5	1.2
24	16	16	1.4	1.0	2.4
12	32	32	2.8	2.0	4.8
6	64	64	5.5	4.1	9.6
3	128	128	11.0	8.2	19.2
Al_2O_3	674				60
Ta_2O_5		835			53.5

[a] Ideal thicknesses calculated from bulk growth rate.

accumulation to inversion and the inversion to accumulation sweeps.

3. Results and discussion

3.1. SEM

Shown in Fig. 2 is a representative cross sectional SEM image of a 10 bilayer Al_2O_3/Ta_2O_5 nanolaminate film with a total thickness of ~200 nm and a target bilayer thickness of ~20 nm. The target bilayer thickness is comparable with the thickness of the 3×19.2 nm bilayer sample. The image shows consistent and discrete layers of Al_2O_3 and Ta_2O_5.

3.2. Dielectric constant

The average dielectric constant was extracted from the slope of a plot of the accumulation capacitance vs. dot area for the three different contact dot sizes. The average relative dielectric constant for each as-deposited film is plotted vs. targeted bilayer thickness in Fig. 3. For reference, the relative dielectric constants measured for as-deposited 60 nm thick pure Al_2O_3 and 53.5 nm thick Ta_2O_5 films ($\kappa Al_2O_3 = 8.9$, $\kappa Ta_2O_5 = 23.9$) are shown as a dotted line and dashed line, respectively. These values of κ are consistent with previously reported values for thin ALD Al_2O_3 films using TMA/H_2O
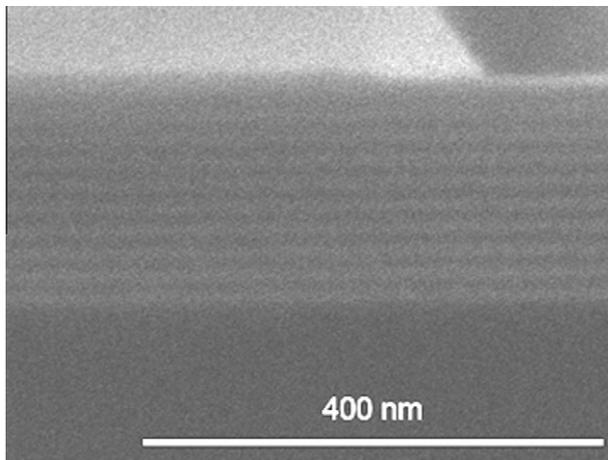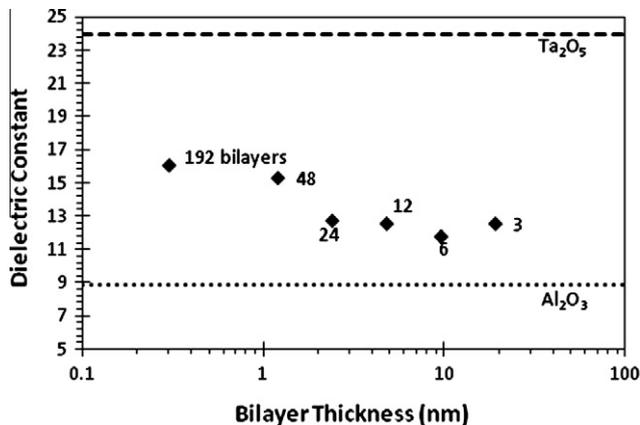
[4,9–11,16–18] and ALD Ta_2O_5 films using $TaCl_5/H_2O$ [1,19]. The relative dielectric constant for the laminate films is seen to range between 12 and 16, with the 192×0.3 nm and 48×1.2 nm films having a higher dielectric constant.

The films of Kattelus et al. [1] that are of a comparable composition to ours (~45% Ta_2O_5 to our ~42% Ta_2O_5) have a dielectric constant of ~12, in line with our few bilayer laminate κ values. The Kattelus et al. film has 30 bilayers and a bilayer thickness of 3.6 nm, similar to the 12×4.8 nm and 24×2.4 nm bilayer films in this work. In order to reach a κ value of 16, comparable to our many bilayer films, Kattelus needed to increase the Ta_2O_5 content to 75%, well above our 42%. This high κ (75% Ta_2O_5) content film had 40 bilayers and a bilayer and individual layer thicknesses comparable to our 24×2.4 nm thick bilayer film. One possible explanation for the lower κ values reported by Kattelus et al. could be the use of chlorine based precursors. Kukli et al. saw that using chlorine free organometallic precursors decreased leakage and by using two organometallic precursors were able to obtain a κ of 15 for a roughly 42% Ta_2O_5 film with 20 nm bilayers and a total thickness near 200 nm [2]. Although the samples in the present work were prepared with a chlorine based tantalum precursor, an organometallic aluminum precursor was used.

Fig. 4 displays the effect of annealing on dielectric constant. A 10 min 400 °C anneal in Ar seemed to null any effect that the number of bilayers/bilayer thickness had for the unannealed films. Little difference was observed between the 400 °C and the 700 °C annealed samples. After the 800 °C anneal, dielectric constant increased in the very thin/many bilayer samples and the 900 °C anneal appeared to increase the dielectric constant for all samples, especially those with the thinnest/most bilayers. The pure Ta_2O_5 samples became very leaky after the 700 °C anneal, making reliable capacitance voltage measurements difficult. The 700 °C anneal coincides with the onset of crystallization in the pure Ta_2O_5 film, as discussed in Section 3.7.

3.3. Hysteresis and V_{fb}

Shown in Fig. 5 is a plot of average hysteresis, ΔV_{hys}, vs. bilayer thickness for as-deposited and annealed samples. The as-deposited samples exhibit counter-clockwise hysteresis during inversion-accumulation-inversion CV sweeps. After a 400 °C anneal, hysteresis is seen to increase in magnitude in the laminates. For samples annealed at 700 °C and above, the magnitude of the hysteresis decreases towards zero and reaches a minimum at 900 °C for most films.

Average flat band (V_{fb}) voltage for an inversion to accumulation CV sweep is plotted in Fig. 6 against the bilayer thickness for various anneal temperatures. For comparison, Ta_2O_5 is plotted on the

Fig. 2. SEM cross section of a 200 nm thick 10 bilayer Al_2O_3/Ta_2O_5 ALD nanolaminate.

Fig. 3. Plot of dielectric constant vs. bilayer thickness for as-deposited laminates. The dielectric constant of Al_2O_3 and Ta_2O_5 are shown for reference.
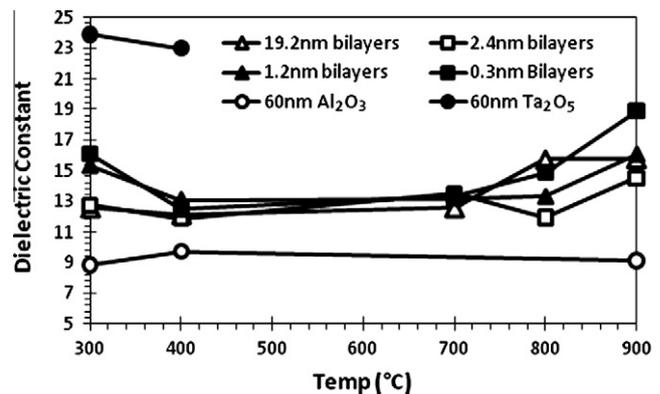
Fig. 4. Plot of dielectric constant as a function of isochronal anneal temperature.
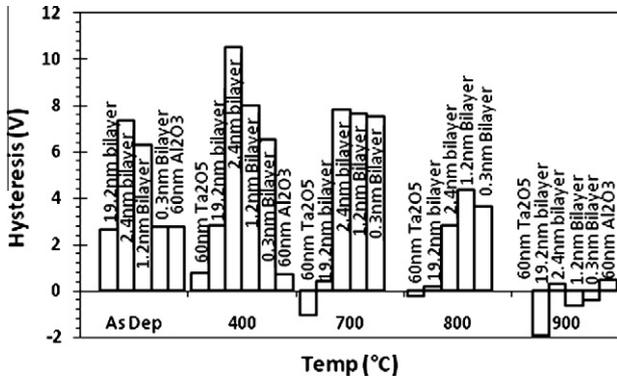
Fig. 5. Comparison of ΔV_{hys} vs. bilayer thickness for as-deposited and annealed films. Counter-clockwise hysteresis is positive.
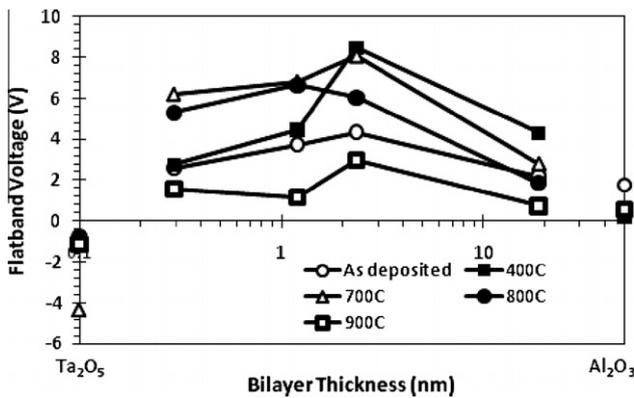
Fig. 6. Plot of average V_{fb} vs. bilayer thickness for as-deposited and annealed films. Pure Ta_2O_5 is plotted on the left, pure Al_2O_3 is plotted on the right.

left at 0.1 nm and Al_2O_3 the right at 50 nm. Ta_2O_5 has a consistently negative V_{fb} while in all other films, V_{fb} is positive. For nearly all temperatures the 24×2.4 nm bilayer sample has the most positive V_{fb}. For all laminates the initial 400 °C anneal increases V_{fb}. V_{fb} of the 3×19.2 nm and 24×2.4 nm bilayer films decreases with further annealing above 400 °C. In the 48×1.2 nm and the 192×0.3 nm bilayer films, V_{fb} peaks positive after the 700 °C anneal and approaches $V_{fb} = 0$ with the 900 °C anneal. V_{fb} of all nanolaminate films is reduced after a 900 °C anneal.

3.4. I–V curves

Shown in Fig. 7 are representative I–V sweeps taken at a sweep rate of 1 MV/cm/s for the as-deposited films. The 192×0.3 nm,
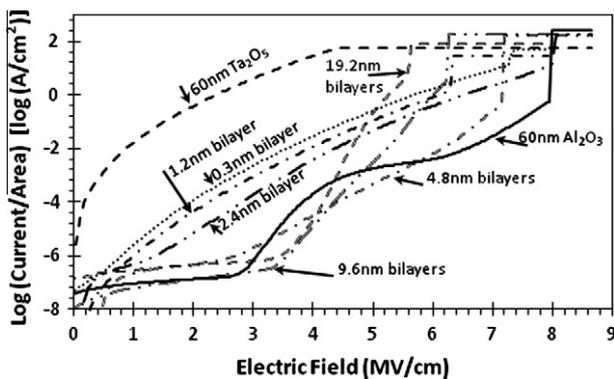
Fig. 7. Representative as-deposited I–V curves of as-deposited films.

48×1.2 nm, and 24×2.4 nm bilayer films have curves similar to Ta_2O_5 while the 3×19.2 nm and 6×9.6 nm bilayer films more closely resemble Al_2O_3, suggesting that there are different conduction mechanisms at play in the different films. The 12×4.8 nm bilayer film seems to be intermediate between the two. Clarification of specific conduction mechanisms will require a comparison of I–V curves as a function of temperature. Note that for fields between 3.5 and 5.5 MV/cm, leakage in the few thick bilayer films (3×19.2 nm, 6×9.6 nm, and 12×4.8 nm) is lower than that of Al_2O_3.

3.5. Leakage

Shown in Fig. 8 is a comparison of median leakage current density at 1 MV/cm for as-deposited and annealed films. The 1 MV/cm leakage of all laminate films is less than for the pure Ta_2O_5 films. At 1 MV/cm the leakage current density in many of the films is near the noise floor of our measurements, however, the leakage of the many bilayer (192×0.3 nm and 48×1.2 nm) films is higher than the few bilayer films. To obtain a comparison above the noise floor, the leakage at 4 MV/cm is plotted in Fig. 9. Though the Ta_2O_5 and the leakiest 900 °C annealed films have currents at compliance (20 μA), the same general trends are observed at 4 MV/cm as at 1 MV/cm. For the as-deposited films, leakage tends higher for the films with many thin bilayers (having many interfaces), a trend that holds with annealing. The 400 °C anneal is seen to decrease leakage in all of the laminate films. Leakage changes little between the 400 °C and the 700 °C annealed samples but increased at 800 °C. After the 900 °C anneal, the leakage in all the films
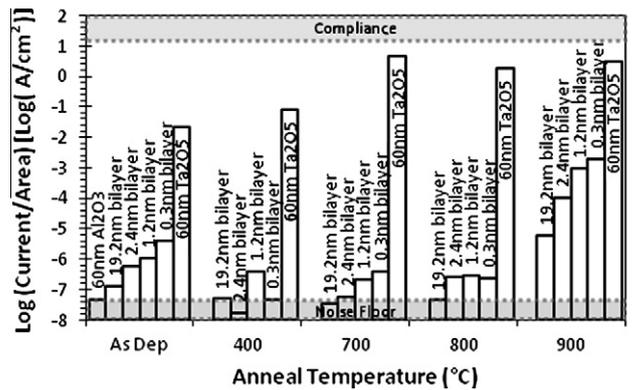
Fig. 8. Comparison of median 1 MV/cm leakage for as-deposited and variously annealed films.
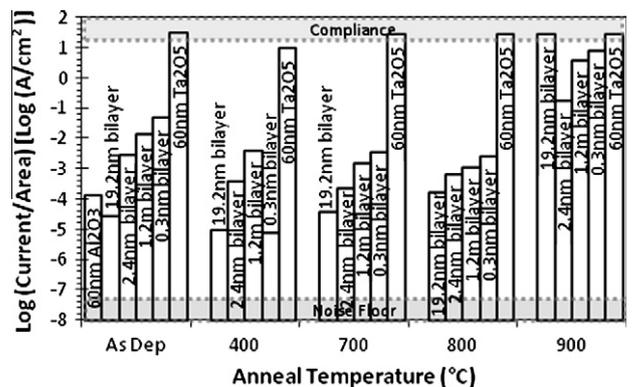
Fig. 9. Comparison of median 4 MV/cm leakage for as-deposited and variously annealed films.

increased dramatically. Leakage in the pure Ta_2O_5 films increases with annealing up to 700 °C after which it reaches the limiting current for the test. The 700 °C anneal coincides with crystallization of the Ta_2O_5 film (discussed in Section 3.7).

3.6. Breakdown

Shown in Fig. 10 is a plot of median ramped breakdown field for as-deposited and annealed films. Breakdown was considered to occur at the voltage where the current showed its first sharp increase in magnitude (as can be seen in Fig. 7), often right to the compliance limited current of 0.2 mA. As dielectric breakdown is well known to be a statistical process, measurements were made on at least six samples and the data points represent the point at which a cumulative 50% of the samples have shown breakdown. Breakdown could not be detected in the pure Ta_2O_5 samples, possibly because these films showed very high leakage (as indicated in by Fig. 7). The as-deposited many/thin bilayer samples (192 × 0.3 nm and 48 × 1.2 nm) show higher breakdown strength than the thick bilayer films (3 × 19.2 nm and 24 × 2.4 nm). Breakdown strength was improved for all laminate films by the 700 °C anneal and was degraded in all films for the 900 °C anneal.

3.7. X-ray diffraction

Shown in Fig. 11 are plots of intensity vs. 2θ for as-deposited and annealed pure Ta_2O_5 films. No long-range order is detected in either as-deposited or 400 °C annealed samples. The strong peaks in the samples annealed at 700 °C and above indicate long-range order is present in these samples and suggest the formation of crystallites. This is consistent with results from literature for

Ta_2O_5 of similar thickness [20–22]. The peaks correspond fairly well to those of base centered orthorhombic Ta_2O_5 [23].

Intensity vs. 2θ diffraction patterns for all films annealed at 700 °C, 800 °C, and 900 °C are shown in Figs. 12–14. As shown in Fig. 14, no long-range order was detected in any of the laminate films annealed at 700 °C and no long-range order was detected in the pure Al2O3 annealed up to 900 °C (Fig. 12). For the 800 °C (Fig. 13) and 900 °C (Fig. 12) annealed laminate films, only the 3 × 19.2 nm bilayer films (which contain 3 × 8.2 nm thick Ta_2O_5 layers) revealed Ta_2O_5 peaks. These Ta_2O_5 peaks are barely visible after the 800 °C anneal and become more pronounced in the 900 °C annealed samples. As seen in Fig. 4, it is at these temperatures that the laminates begin to show a change in dielectric constant. There are several possible explanations for the lack of Ta_2O_5 peaks in the rest of the many bilayer laminate films. One possible explanation is that, as reported by Kukli et al. [2,3] for thin ZrO_2 and HfO_2 layers, crystallization is inhibited in the thin spatially confined Ta_2O_5 layers. However, another explanation for the lack of observed Ta_2O_5 peaks is that they are broadened below our detection limit. While the pure Ta_2O_5 film was ~60 nm thick, the total Ta_2O_5 thickness in the laminate films was only ~29 nm and further split into multiple layers: the Ta_2O_5 layers are ~9.7 nm thick in the 3 × 19.2 nm bilayer films, ~1.2 nm thick in the 24 × 2.4 nm bilayer films, and less than ~0.2 nm thick in the 192 × 0.3 nm bilayer films. The thickness of the individual layers limits the maximum Ta_2O_5 crystallite size, making them more difficult to detect via XRD.

3.8. Figure of merit

In previous work with Ta_2O_5/HfO_2, Ta_2O_5/ZrO_2, and Ta_2O_5/Al_2O_3 laminates, Kukli et al. [2,3] have used a figure of merit to evaluate the suitability of their films as capacitors. They define a charge storage factor, Q, where Q = UcrC/S, Ucr is the voltage required to induce 1 uA/cm^2 of leakage, C is the accumulation capacitance, and S is the surface area of the device. A cumulative plot charge storage factor for select films is plotted in Fig. 15. The as-deposited few thick bilayer films, were found to have the highest Q-values: the 6 × 9.6 nm bilayer film was highest, followed closely by the 3 × 19.2 nm and 12 × 4.8 nm bilayer films. A similar trend is seen in the Kukli et al. work with ZrO_2/Ta_2O_5 laminates. The 900 °C annealed 192 × 0.3 nm bilayer and pure Ta_2O_5 films have the lowest Q-values. The pure Al2O3 film has a Q of ~24 nC/mm^2, higher than the 15 nC/mm^2 reported by Kukli et al. for a thicker pure Al_2O_3 film that was also deposited using TMA and H_2O. On the other hand, the Kukli et al. pure Ta_2O_5 was slightly higher than that reported here, 6 nC/mm^2 compared to our ~1 nC/mm^2. Rather than the $TaCl_5$ precursor used in this work, Kukli et al. used tantalum ethoxide, $Ta(OC_2H_5)_5$, which decreased the leakage of their pure Ta_2O_5 films
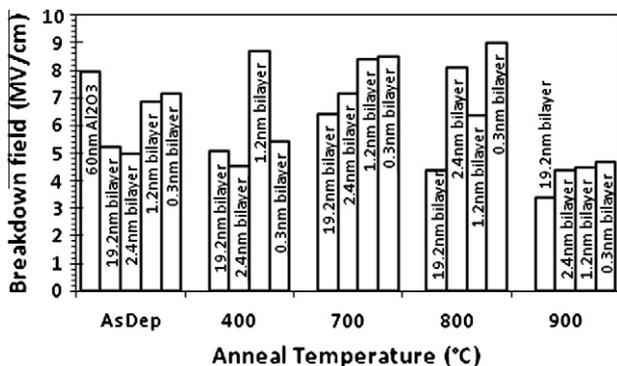
Fig. 10. Comparison of median ramped breakdown voltage for as-deposited and variously annealed films.
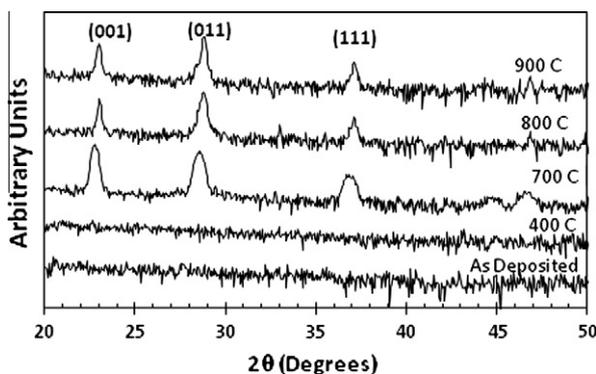
Fig. 11. XRD plot of arbitrary log intensity vs. 2ϑ for as-deposited and annealed ~60 nm thick Ta_2O_5 films. Ref. Pattern 01-089-2843.
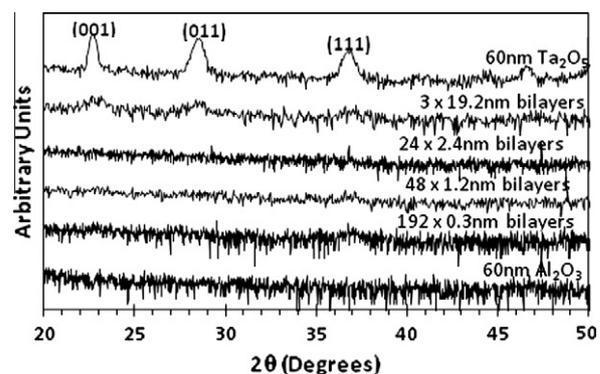
Fig. 12. XRD plot of arbitrary log intensity vs. 2ϑ for 900 °C annealed films. Ref. Pattern 01-089-2843.
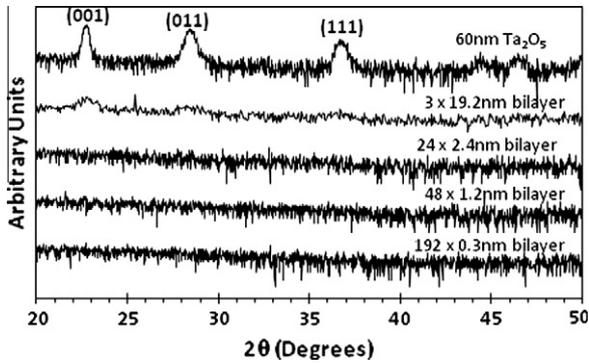
Fig. 13. XRD plot of arbitrary log intensity vs. 2ϑ for 800 °C annealed films. Ref. Pattern 01-089-2843.
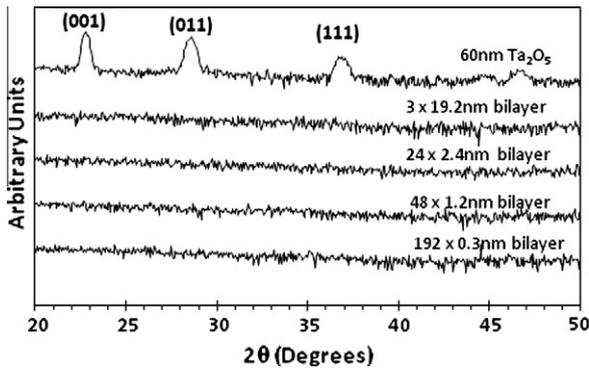
Fig. 14. XRD plot of arbitrary log intensity vs. 2ϑ for 700 °C annealed films. Ref. Pattern 01-089-2843.
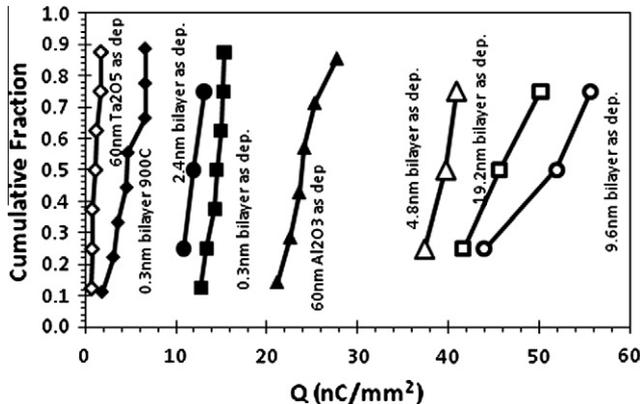
Fig. 15. Cumulative fraction plot of the charge storage factor, Q, for select films.

by roughly an order of magnitude relative to the films produced in this study and in Kattelus et al. [1]. For approximately 200 nm thick Al_2O_3–Ta_2O_5 laminates of various compositions but with a consistent bilayer thickness of ~20 nm, Kukli et al. reported a Q value of ~30 nC/mm^2. The most similar laminate film in this study, the 3×19.2 nm bilayer films, had a Q in the range of 40–50 nC/mm^2. Our film's higher Q value is due to its lower leakage current, having a Ucr ~150% that of Kukli et al. This outweighs the benefit of the slightly higher κ (~15 vs. our ~12) would have for the C. Overall, the films in this study exhibited Q-values from ~5 nC/mm^2 to ~50 nC/mm^2, suggesting that even for a fixed overall composition, the number and thickness of bilayers may be used to tune dielectric properties.

4. Conclusion

Amorphous Ta_2O_5–Al_2O_3 laminates were deposited via ALD using $Al(CH_3)_3$ and $TaCl_5$ as metal precursors with water as an oxidant. By using a fixed total thickness and overall composition ratio and varying only the numbers of Ta_2O_5/Al_2O_3 bilayers, the impact of the bilayer thickness and the total number of interfaces on dielectric properties is investigated without interference from changes in overall composition or crystal structure. The total target thickness was 58 nm and the overall composition was fixed at approximately 57% Al_2O_3/43% Ta_2O_5, based on the bilayer thickness ratio. The number (thickness) of bilayer ranged from 3 (19.2 nm) to 192 (0.3 nm). The thickness of the films studied (~58 nm) is relevant to gate dielectric applications in amorphous oxide semiconductor TFTs in which an SiO_2 equivalent thickness of ~100 nm is typically required [12,13]. It was found that despite the fixed overall target composition, varying the number/thickness of the bilayers had an impact on electrical properties. While almost all samples exhibited breakdown and leakage intermediate between single layer Al_2O_3 or Ta_2O_5 films, samples with thinner (more numerous) bilayers tended towards higher effective dielectric constant, but higher leakage current than few (thick) bilayer samples. Several of the samples with fewer (thicker) bilayers exhibited leakage current density even lower than that of Al_2O_3 over the range of ~3.5–4.5 MV/cm. To explore the influence of crystallization on the laminates, select samples were annealed in an inert atmosphere. Annealing laminates at low temperatures improved leakage and breakdown while higher temperature anneals degraded both leakage and breakdown but improved the effective dielectric constant.

Comparing the samples using a charge storage figure of merit [2,3] revealed the few (thick) bilayer films to be ranked higher than the many bilayer laminates as well as both the pure Ta_2O_5 and pure Al_2O_3 films. These results indicate that for a fixed overall composition, varying the number of bilayers may be used to tailor the electrical properties of a nanolaminate dielectric.

References

[1] Kattelus H, Ylilammi M, Saarilahti J, Antson J, Lindfors S. Layered tantalum–aluminum oxide films deposited by atomic layer epitaxy. Thin Solid Films 1993;225(1–2):296–8.
[2] Kukli K, Ihanus J, Ritala M, Leskela M. Properties of Ta_2O_5-based dielectric nanolaminates deposited by atomic layer epitaxy. J Electrochem Soc 1997;144(1):300–6.
[3] Kukli K, Ihanus J, Ritala M, Leskela M. Tailoring the dielectric properties of HfO_2–Ta_2O_5 nanolaminates. Appl Phys Lett 1996;68(26):3737–9.
[4] Zhang H, Solanki R, Roberds B, Bai S, Banerjee I. High permittivity thin film nanolamintes. J Appl Phys 2000;87:1921.
[5] Sechrist ZA, Fabreguette FH, Heintz O, Phung TM, Johnson DC, George SM. Chem Mater 2005;17:3475.
[6] Jenson JM, Oelkers AB, Toivola R, Johnson DC, Elam JW, George SM. Chem Mater 2002;14:2276.
[7] Zhong L, Daniel WL, Zhang Z, Campbell S, Gladfelter WL. Chem Vapor Depos 2002;12:143.
[8] Conley Jr JF, Ono Y, Tweet DJ. Appl Phys Lett 2004;84(11):1913.
[9] Conley Jr JF, Ono Y, Tweet DJ, Solanki R. Appl Phys Lett 2004;84(3):398.

[10] Huang CC, Cann DP. Phase transitions and dielectric properties in Bi(Zn1/2Ti1/2)O$_3$-BaTiO$_3$ perovskite solid solutions. J Appl Phys 2008;104(2):024117.

[11] Wang X, Liu J, Bai W, Kwong DL. A novel MONOS-type memory using high-k dielectrics for improved data retention and programming speed. IEEE Trans Electron Dev 2004;51(4):597–602.

[12] Wager JF, Keszler DA, Presley RA. Transparent electronics. New York: Springer; 2008.

[13] Chang S, Song YW, Lee S, Lee SY, Ju BK. Efficient suppression of charge trapping in ZnO-based transparent thin film transistors with novel Al$_2$O$_3$/HfO$_2$/Al$_2$O$_3$ structure. Appl Phys Lett 2008;92(19):192104.

[14] Puurunen R. J Appl Phys 2005;97(12):1301.

[15] Ritala M, Leskela M. Handbook of thin film materials, vol. 1. 2002. p. 103.

[16] Groner MD, Elam JW, Fabreguette FH, George SM. Electrical characterization of thin Al2O3 films grown by atomic layer deposition on silicon and various metal substrates. Thin Solid Films 2002;413(1–2):186–97.

[17] Wilk GD, Wallace RM, Anthony JM. High-k gate dielectrics: current status and materials properties considerations. J Appl Phys 2001;89(10):5243–75.

[18] Conley Jr JF, Ono Y, Tweet DJ, Zhuang W, Solanki R. Atomic layer deposition of thin hafnium oxide films using a carbon free precursor. J Appl Phys 2003;93(1):712–8.

[19] Zhang J, Lim B, Boyd IW. Deposition and annealing of tantalum pentoxide films using 172 nm excimer lamp. Appl Surf Sci 2000;154–155:382–6.

[20] Wu SJ, Houng B, Huang B. Effect of growth and annealing temperatures on the crystallization of tantalum pentoxide thin film prepared by RF magnetron sputtering method. J Alloys Compd 2009;475:488–93.

[21] Park SW, Baek YK, Lee JY, Park CO, Im HB. Effects of annealing conditions on the properties of tantalum oxide films on silicon substrates. J Electron Mater 1992;21(6):635–9.

[22] He X, Wu J, Li X, Gao X, Gan X, Zhao L. J Alloys Comp 2009;478:453–7.

[23] Lehvic K. J Less-Common Met 1964;27:1037.